Electronic Supplementary Information

Low-costs CoFe₂O₄/Biomass Carbon Hybrid from metal-enriched Sulfate Reducing Bacteria as Electrocatalyst for Water Oxidation

Songhu Bi [a], Jingde Li [b], Qing Zhong [b], Chuntan Chen [c,d], Qiyi Zhang [a] * and Yongyi Yao [b]

[a] School of Chemical Engineering, Sichuan University, Chengdu, Sichuan, 610065, P. R. China.

[b] Textile College, Sichuan University, Chengdu, Sichuan, 610065, P. R. China.

[c] Chengdu Ketai Tech Co., Ltd, Chengdu, Sichuan, 610065, P. R. China.

[d] School of Chemistry and Chemical Engineering, Sichuan University of Arts and Science, Dazhou, Sichuan, 635000, P. R. China.

[*] Corresponding authors′ e-mail: qyzhang-scu@163.com

Theoretical calculations： In this paper, the Vienna ab initio simulation package (VASP) in the framework of the projector augmented wave (PAW) method was used for all calculations. The cutoff for the plane waves set as 520 eV. Hubbard-like, localized term was added to the PBE generalized gradient approximation (GGA) exchange correlation functional, called GGA+U. The Ueff (U-J) value of 4.5 eV was applied for both Co 3d and Fe 3d states. All 2×2×2 supercells with 4×4×2 mesh of k-points were used to calculate the electronic structure of CoFe₂O₄. For calculations of adsorption energy, (100) surfaces were modeled using symmetric slabs of one layer with vacuum widths of 10 Å. All atoms were fully relaxed with the energy convergence tolerance of 10^{-6} eV/atom, and the final force on each atom was < 0.01 eV/Å. And the adsorption energies of OH⁻ (E^{OH-}) and O₂ (E^{O_2}) on surfaces of CoFe₂O₄ were calculated based on the following formula:

$$E^{(OH-)} = E(OH^-) + E(SUR) - E(SUR + OH^-) \tag{1}$$

$$E^{(O_2)} = E(O_2) + E(SUR) - E(SUR + O_2) \tag{2}$$

Where E (SUR), E (SUR+OH⁻) and E (SUR +O₂), $E^{(OH-)}$, $E^{(O_2)}$ were denoted the total energies of the metal oxide surfaces, OH⁻, O₂ and metal oxide surfaces adsorbed with OH⁻ and O₂, respectively.

And the reaction mechanism were calculated based on the following formula:

$$\Delta E_{OH} = E(OH^*) - E(^*) - [E(H_2O) - 1/2\,E(H_2)] \tag{3}$$

$$\Delta E_O = E(O^*) - E(^*) - [E(H_2O) - E(H_2)] \tag{4}$$

$$\Delta E_{OOH} = E(OOH^*) - E(^*) - [2E(H_2O) - 3/2\,E(H_2)] \tag{5}$$

$$\Delta G_i = \Delta E_i + \Delta ZPE_i - T\Delta S_i \tag{6}$$

And the ($\Delta ZPE_i - T\Delta S_i$) of O*, OH* and OOH* was 0.07, 0.37 and 0.44 eV, respectively [R19].

$$\Delta GH^+(pH) = -k_B T \ln(10) \times pH. \tag{7}$$

k_B was the Boltzmann constant.

$$\Delta G1 = \Delta GOH - eU + \Delta GH^+(pH) \tag{8}$$

$$\Delta G2 = \Delta GO - \Delta GOH - eU + \Delta GH^+(pH) \tag{9}$$

$$\Delta G3 = \Delta GOOH - \Delta GO - eU + \Delta GH^+(pH) \tag{10}$$

$$\Delta G4 = 4.92\,[eV] - \Delta GOOH - eU + \Delta GH^+(pH) \tag{11}$$

$$\eta(over) = \max\{\Delta G1, \Delta G2, \Delta G3, \Delta G4,\}/e - 1.23V \tag{12}$$

Determination of morphology factors: Since we could not obtain the value of theoretical double-layer capacitance of cobalt ferrite and 60~80 μFcm^{-2} was usually used as the theoretical value of metallic oxide,[37] morphology factor (φ), a more accurate value was used to characterize the active site for metallic oxide. Normally, roughness and/or porosity factors are used to describe the non-planarity of the surface of solid electrodes. In the case of the roughness factor, the experimental capacity is divided by the theoretical value of a well-defined planar surface.

The detailed information on the double-layer capacitor current comes from reference 38, where there is a detailed proof of the process.

$$C_d = \left(\frac{di_c}{d\upsilon}\right)_E \tag{13}$$

$$C_i = C_d - C_e \tag{14}$$

$$\varphi = \frac{C_i}{C_d} \tag{15}$$

Where φ was the morphology factor. C_e (fast scan rate) and C_i are the external capacitor and the internal capacitor. C_d is the double-layer capacitance under slow scan rate.
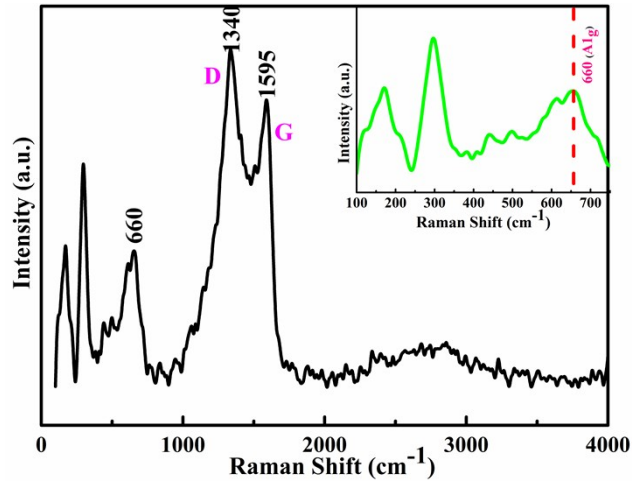
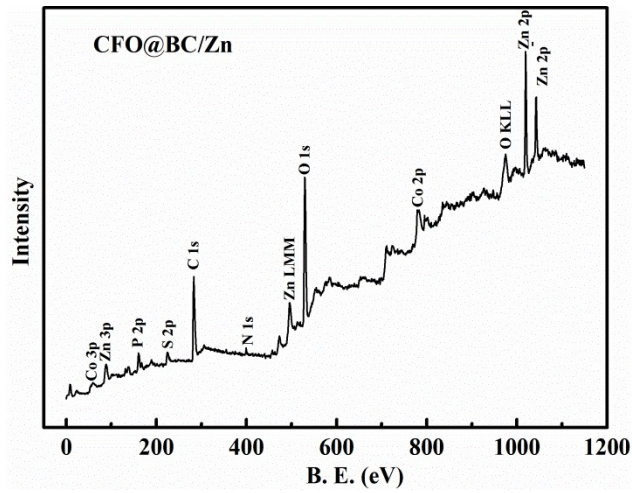**Figure s1.** Raman pattern of CFO@BC/Zn hybrid.
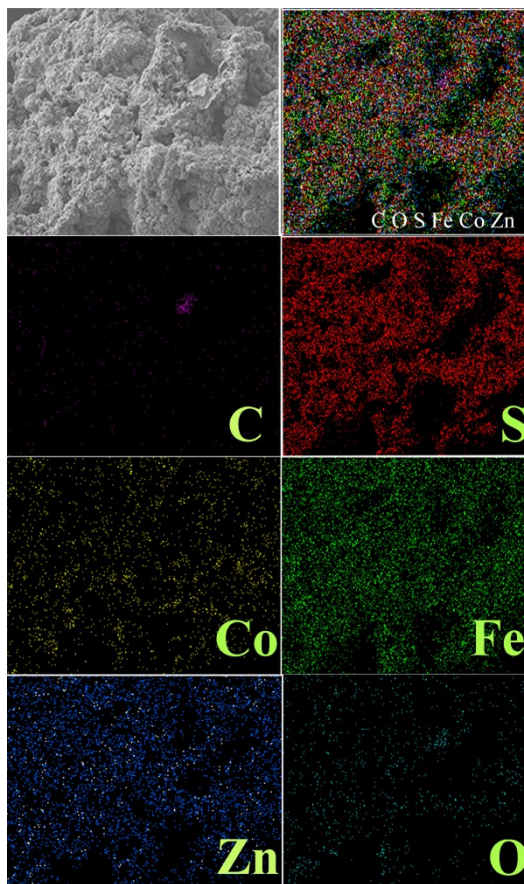

Figure s2. XPS pattern of CFO@BC/Zn hybrid.

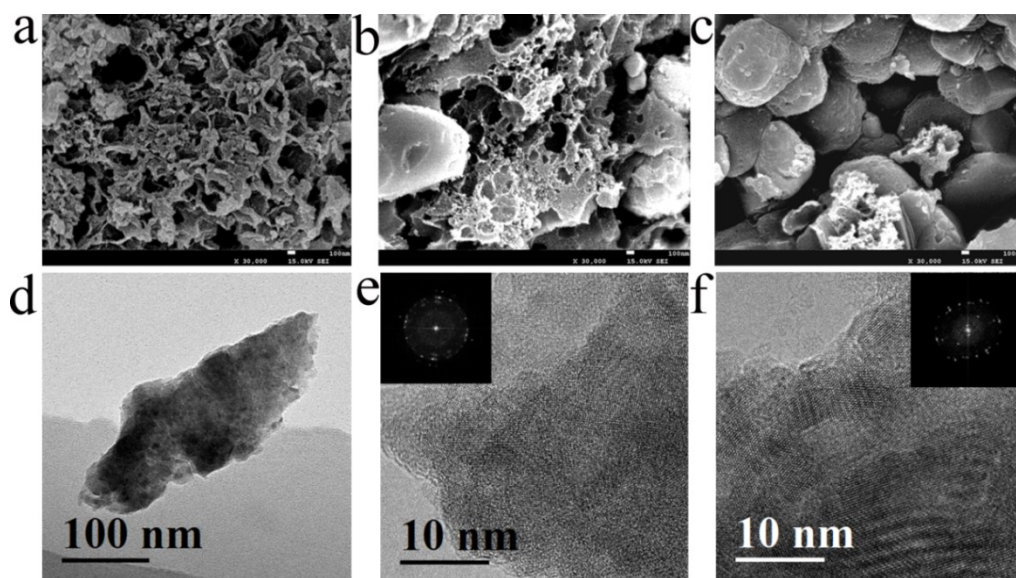**Figure s3.** EDS map of CFO@BC/Zn including Co, Fe, O, S, C, and Zn elements.
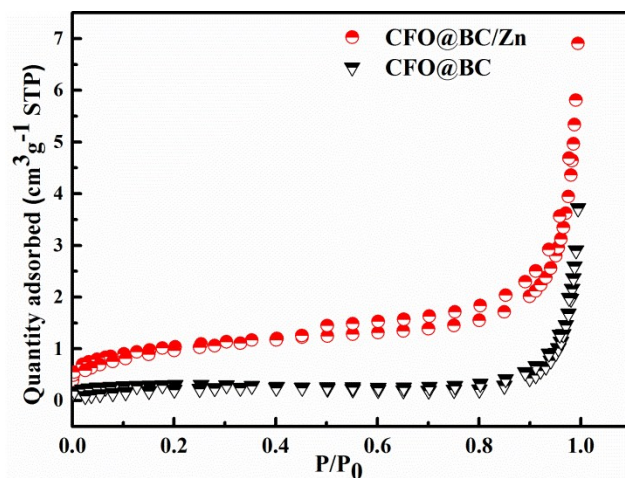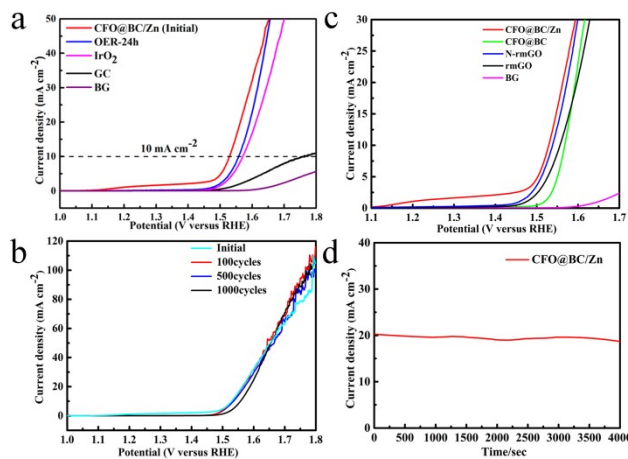

Figure s4. (a) SEM images of freeze-dried SRB; (b) and (c) were SEM images of CFO@BC/Zn, showing porous structure and rough surface; (d), (e) and (f) were TEM and HRTEM images of ZnS

Figure S5. The N2 physisorption isotherms were obatained by Brunauer–Emmett–Teller method. The sample was first heated at 120 ° C for 2 hours to remove moisture and then activated at 300 ° C for 3 hours.
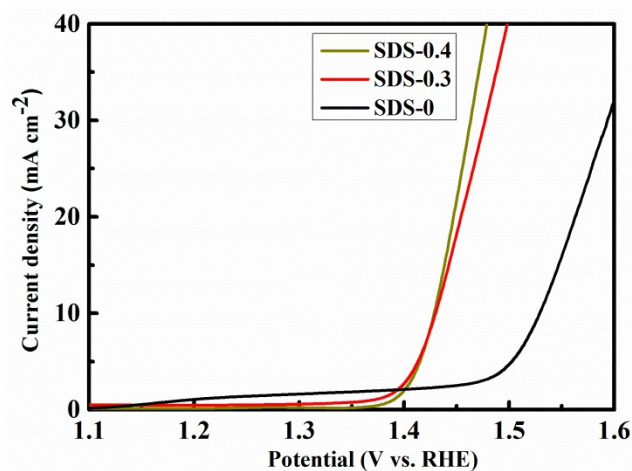

Figure s6. (a) LSV curves of CFO@BC/Zn hybrid, after performed OER for 24 h and (BG), IrO$_2$, GC. (b) LSV curves of CFO@BC/Zn, CFO@BC, Co$_3$O$_4$/N-rmGO, Co$_3$O$_4$/rmGO hybrid and (BG). (c) LSV curves about CFO@BC/Zn of initial, after 100cycles, after 500 cycles and after 1000 cycles. (d) time dependence of the current density under a constant potential 1.52 V of CFO@BC/Zn hybrid supported on foam Ni.
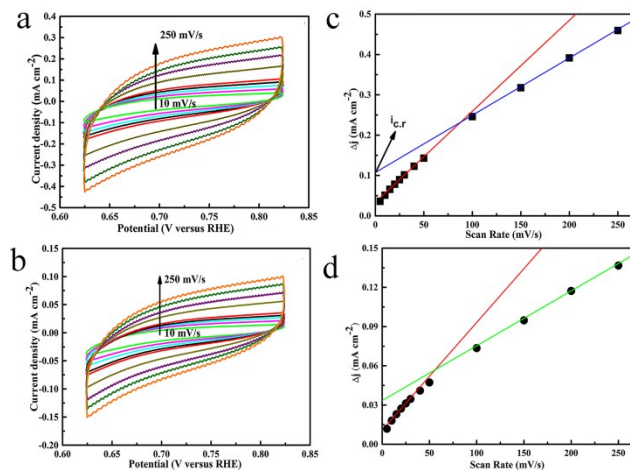
Figure s7. (a) CV curves of CFO@BC/Zn from 10 mV/s to 50 mV/s, and charging current density differences ($\Delta j = j_a - j_c$) at 0.724 V vs. RHE, (b) CV curves of CFO@BC, (c) charging current density differences ($\Delta j = j_a - j_c$) at 0.724 V vs. RHE plotted against the scan rate. (c) Dependence of the capacitive voltammetric current ($\Delta j = j_a - j_c$) at 0.724 V vs RHE of CFO@BC/Zn. (d) Dependence of the capacitive voltammetric current ($\Delta j = j_a - j_c$) at 0.724 V vs RHE of CFO@BC.

In order to accurate check and characterized the oxide with rough surface, and considered with the surface charging of conductive metallic oxide, we use a morphology factor (φ) to read the difference of electrocatalytic performance. And we obtained the limited diffusion current (Scan rate approach to zero under fast rate). According to the electrochemical double layer theory, the limited diffusion current was produced by the diffusion of ions under fast scan rate, which indicated an easy diffusion of ions on CFO@BC/Zn surfaces.
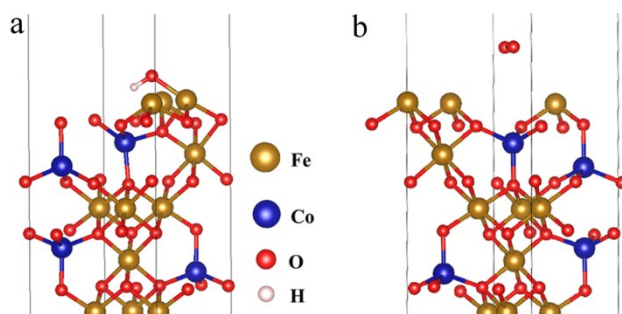

Figure s8. LSV curves of CFO@BC/Zn hybrid in 1M NaOH with SDS (0, 0.3g and 0.4g/100 mL).
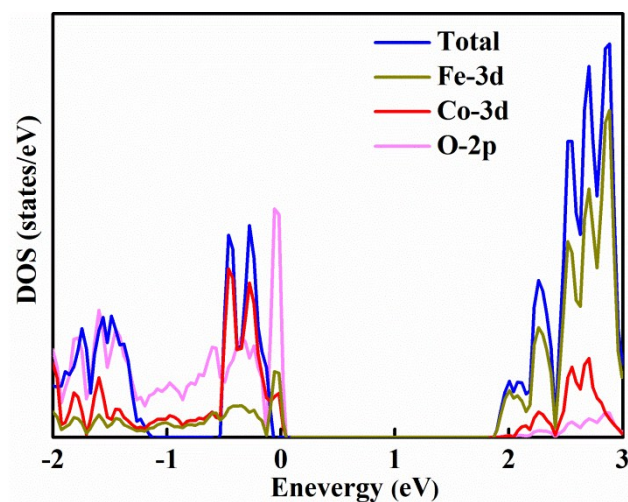
Figure s9. The total DOSs and the projected densities of states (PDOSs) of CFO

Figure s10. (a) adsorption of O_2 on (100) surface of CFO; (b) adsorption of OH^- on (100) surface of CFO.

Table S1. Comparison of OER activity of the CFO@BC/Zn hybrid with recently reported catalysts.

Electrocatalyst	Mass loading (mg·cm⁻²)	Electrolyte	Potential vs RHE at 10 mA·cm⁻² (V)	Substrate	Reference
CFO@BC/Zn	0.34	1.0 M NaOH	1.53	GC	This work
R-CFO@BC/Zn	0.34	1.0 M NaOH	1.47	GC	This work
CFO@BC/Zn	2.5	1.0 M NaOH	1.45	Ni foam	This work
Co-P	2.71	1 M KOH	1.57	Cu foil	S 1
CoO/CNF	N	0.1 M KOH	1.57	CFP	S 2

Co(OH)$_2$	N	1 M KOH	1.557	GC	R 32
N-CG–CoO	0.34	1 M KOH	1.57	GC	R 14
Ni$_x$Co$_{3-x}$O$_4$	2.7	1 M NaOH	1.65	Ti foil	S 3
Co$_3$O$_4$/N-rmGO	0.1	1 M NaOH	1.54	GC	R 17
Co(PO$_3$)$_2$	1.1	PBS	1.635	Ni foam	S 4
Mn$_3$O$_4$/CoSe$_2$	0.2	0.1 M KOH	1.68	GC	S 5
CeO$_2$/CoSe$_2$	0.2	0.1 M KOH	1.518	CFP	S 6
NiFeO$_x$	N	1 M NaOH	1.58	GC	R 16
Fe-Co$_3$O$_4$	0.12	0.1 M KOH	1.71	GC	S 7
Ni$_3$N	0.285	1 M KOH	1.57 (52.3 mA·cm$^-$	Carbon cloth	S 8
CoO$_x$@CN	2.1	1 M KOH	1.55 (20 mA·cm^{-2})	Ni foam	R 13
CoMnO@CN	N	1 M KOH	1.65 (308 mA·cm^{-2})	Ni foam	R 21

References

S 1 N. Jiang, B. Y. M. Sheng, Y. Sun. Angew. Chem. 2015**,** 127, 6349.
S 2 H. Wang, H. Lee, Y. Deng, Z. Lu, P. Hsu, Y. Liu, D. Lin, Y. Cui. Nat. Commun. 2015**,** 6, 7261.
S 3 Y. Li, H. Panitat, Y. Wu. Adv. Mater. 2010**,** 22, 1926.
S 4 S. A. Hyun, T. T. Don. Adv. Funct. Mater. 2013**,** 23, 227.
S 5 M. Gao, Y. Xu, J. Jiang, Y. Zheng, S. Yu. J. Am. Chem.Soc. 2012**,** 134, 2930.
S 6 Y. Zheng, M. Gao, Q. Gao, H. Li, J. Xu, Z. Wu, S. Yu. Small**.** 2015**,** 11,182.
S 7 G. Tobias, X. Deng, T. Harun. Chem. Mater. 2014**,** 26, 3162.
S 8 J. Wang, D. Gao, G. Wang, S. Miao, H. Wu, J. Li, X. Bao. J Mater Chem. A. 2014**,** 2, 20067.